Improved the AlGaN-Based Ultraviolet LEDs Performance With Super-Lattice Structure Last Barrier

Volume 10, Number 4, August 2018

Qian Chen
Jun Zhang
Yang Gao
Jingwen Chen
Hanling Long
Jiangnan Dai
Zi-hui Zhang
Changqing Chen

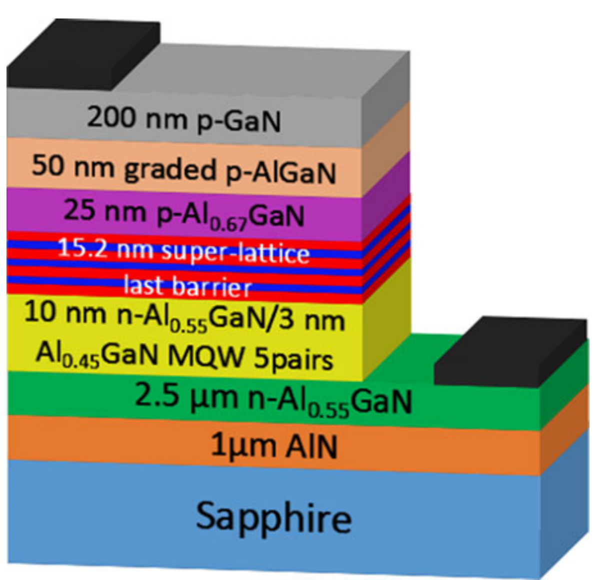

DOI: 10.1109/JPHOT.2018.2852660
1943-0655 © 2018 IEEE

Improved the AlGaN-Based Ultraviolet LEDs Performance With Super-Lattice Structure Last Barrier

Qian Chen,[1] Jun Zhang,[1] Yang Gao,[1] Jingwen Chen,[1] Hanling Long,[1] Jiangnan Dai,[1] Zi-hui Zhang,[2] and Changqing Chen[1]

[1]Wuhan National Laboratory for Optoelectronics, Huazhong University of Science and Technology, Wuhan 430074, China
[2]Institute of Micro-Nano Photoelectron and Electromagnetic Technology Innovation, Electronics and Information Engineering, Hebei University of Technology, Tianjin 300401, China

DOI:10.1109/JPHOT.2018.2852660
1943-0655 © 2018 IEEE. Translations and content mining are permitted for academic research only. Personal use is also permitted, but republication/redistribution requires IEEE permission. See http://www.ieee.org/publications standards/publications/rights/index.html for more information.

Manuscript received March 14, 2018; revised June 23, 2018; accepted June 28, 2018. Date of publication July 3, 2018; date of current version July 18, 2018. This work was supported in part by the Key Project of Chinese National Development Programs under Grants 2016YFB0400901 and 2016YFB0400804, in part by the National Natural Science Foundation of China under Grants 61675079, 11574166, 61377034, 61774065, and 61704062, in part by the Director Fund of WNLO, and in part by the China Postdoctoral Foundation under Grant 2016M602287. Corresponding author: Jiangnan Dai (e-mail: daijiangnan@hust.edu.cn).

Abstract: In this paper, a structure of super-lattice structure last barrier (SLSLB) is proposed, which can be applied into the AlGaN-based ultraviolet light-emitting diodes (LEDs) for improving the injection of both electrons and holes. Several other SLSLBs are also designed and compared in this work, and according to the simulated results, we find that the LED with SLSLB of diminishing thickness (SLSLB-D) possesses the highest internal quantum efficiency and the smallest efficiency droop. The SLSLB-D can effectively reduce the electron concentration at the interface between the last barrier (LB) and electron block layer (EBL), which relieves the leakage of electrons. Moreover, the best hole injection capability for the LED with SLSLB-D also contributes to the improved optical performance.

Index Terms: Super-lattice last barrier, ultraviolet light-emitting diode, efficiency droop alleviation.

1. Introduction

In recent years, the AlGaN-based deep ultraviolet light-emitting diodes (DUV-LEDs) have attracted more and more attention because they possess great potential application in many fields, such as water purification, air sterilization, full-color displays, chemical sensors, and medical applications [1]–[4]. Nowadays, the DUV LED performance is still lower than satisfaction and far away from the commercialization. The low internal quantum efficiency (IQE) is an important factor restricting the performance of DUV LEDs [5]–[7]. Several obstacles have been taken account for the low IQE of DUV LEDs. Firstly, the lattice and thermal mismatches between Al-rich AlGaN layers and sapphire substrate lead to a very high threading dislocation density (TDD) that is in the order of $10^9 - 10^{10}\,cm^{-2}$ for the subsequently grown epi-layer [8], [9]. The high TDD seriously affects the recombination efficiency of carriers. Secondly, the effects of huge built-in electric fields caused by the spontaneous and piezoelectric polarization bends the energy band of quantum wells, and

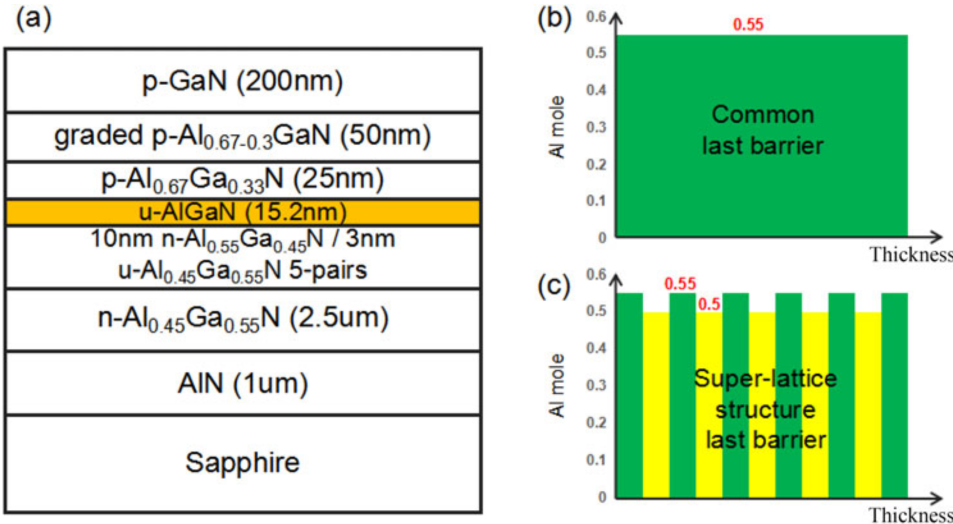

Fig. 1. (a) Schematic DUV LED structure. (b) schematic energy band diagrams for common last barrier $Al_{0.55}Ga_{0.45}N$ layer with undoped of 15.2 nm, and (c) schematic energy band diagrams for SLSLBs with the total thickness of 15.2 nm for which the detailed information can be found in Table 1.

therefore a reduced wave functions overlap level for electron and hole wave functions. The spatial separation for electron and hole wave functions is known as quantum confined Stark effect (QCSE) [10], [11]. Lastly, seriously electron leakage causes the reduction of the electron concentration in quantum wells [12], [13]. Targeting at solving the above problems, Hirayama *et al.* have come up with the “ammonia (NH_3) pulsed-flow multilayer growth” method to fabricating the AlN template on the sapphire for reducing the TDD to the order of 10^8 cm^{-2} [14]. Tian *et al.* applied the an AlN intermediate layer on the growth of AlN grown process, which can achieved the AlN layer with good morphology and high quality [15]. Tian *et al.* suggested that the quantum barriers with appropriate Si doping concentration to screen the polarization induced electric field and relieve the band bending within the quantum wells [16]. Zhang *et al.* propose inserting p-AlGaN thin layer between the last barrier (LB) and electron blocking barrier (EBL) to regulate the carriers transport, and by doing so, the electron leakage can be alleviated [17].

It is widely believed that relieving the electron leakage and enhancing the hole injection are important to improve the performance for DUV LEDs, and the alternative design of LB next to the Mg-doped layer has been considered as one of the useful strategies since the LB can affect effective barrier of the p-EBL for electron and hole simultaneously. In order to reduce the electron leakage and enhance the hole injection efficiency, many novel LB structures have been proposed [18]–[20]. Recently, Hirayama *et al.* propose adopting the multi-quantum EBL to significantly improved the electron leakage and the enhancement of IQE is obtained experimentally [21]. In this work, we proposed a super-lattice structure last barrier (SLSLB) to replace the traditional last barrier to better increase the electron and hole injections for DUV LEDs. Furthermore, we also explore the effect of different SLSLBs with thickness variation designs on DUV LED performance. The energy band and carrier concentration were numerically investigated by using the Crosslight APSYS (Advance Physical Model of Semiconductor Devices) programs [22], [23]. The APSYS is capable of dealing with Poisson’s equations, current continuity equations, and Schrodinger equation. It is found that the DUV LED with SLSLB of diminishing thickness (SLSLB-D) has the optimal optical power and lowest efficiency droop.

2. Structures and Parameters

The structure of the DUV LED is shown in Fig. 1(a). The DUV LED is grown on a c-plane sapphire substrate, then followed by 1-μm-thick undoped AlN layer. The 2.5-μm-thick Si-doped $Al_{0.45}Ga_{0.55}N$

Table 1
Thickness of Each Quantum Barrier and Quantum Well for Different MQLBs

	QB/nm	QW/nm	QB/nm	QW/nm	QB/nm	QW/nm	QB/nm	QW/nm	QB/nm	QW/nm	QB/nm
SLSLB-I	1.2	1	1.4	1	1.6	1	1.8	1	2	1	2.2
SLSLB-E	1.7	1	1.7	1	1.7	1	1.7	1	1.7	1	1.7
SLSLB-D	2.2	1	2	1	1.8	1	1.6	1	1.4	1	1.2

(Si doping $= 5 \times 10^{18}$ cm^{-3}) electron injection layer is on the AlN layer. The active region includes five 3-nm-thick undoped $Al_{0.45}Ga_{0.55}N$ quantum wells (QWs) that generate the 285 nm peak emission wavelength. The QWs are separated by four 10-nm-thick Si-doped $Al_{0.55}Ga_{0.45}N$ layer (Si doping $= 5 \times 10^{18}$ cm^{-3}). The last barrier is 15.2 nm thick and kept undoped. Note, the only distinction of all structures is the last barrier. We define the undoped 15.2-nm-thick $Al_{0.55}Ga_{0.45}N$ last barrier layer as the reference. We use $Al_{0.55}Ga_{0.45}N/Al_{0.50}Ga_{0.50}N$ super-lattice structure last barrier to replace the $Al_{0.55}Ga_{0.45}N$ last barrier. All $Al_{0.55}Ga_{0.45}N/Al_{0.50}Ga_{0.50}N$ SLSLBs have the same total thickness of 15.2 nm and the same $Al_{0.50}Ga_{0.50}N$ thickness of 1 nm except that the $Al_{0.55}Ga_{0.45}N$ layer thickness varies to three types. One design is that the barrier thickness of the SLSLB increase from 1.2 to 2.2 nm with the step of 0.2 nm (SLSLB-I), another design is that the $Al_{0.55}Ga_{0.45}N$ barrier thickness of the MQLB is 1.7 nm (SLLB-E), the other one is that the $Al_{0.55}Ga_{0.45}N$ barrier thickness of the SLLB diminishes from 2.2 to 1.2 nm with the step of 0.2 nm (SLSLB-D). Even more detailed structure information for the SLSLBs is listed in Table 1. Then a 25-nm-thick Mg-doped $Al_{0.67}Ga_{0.33}N$ EBL (Mg doping $= 5 \times 10^{18}$ cm^{-3}) is on the top of the active region, which is covered by a 50-nm-thick graded Mg-doped $Al_{0.67-0.30}Ga_{0.33-0.70}N$ (Mg doping $= 5 \times 10^{18}$ cm^{-3}) and a 200-nm-thick Mg-doped GaN (Mg doping $= 3 \times 10^{19}$ cm^{-3}) contact layer as the hole injection layer. The device geometry is designed as a square shape of 200×200 μm^2 in size. The Mg dopant ionization efficiency in this program is set to be 1% [24].

During the calculations, the Shockley-Read-Hall (SRH) recombination time is set to be 1.5 ns for all layers [25]. The band-offset ratio is assumed to be 0.7/0.3 for AlGaN materials [26]. The Auger recombination coefficient is set to be 1×10^{-30} cm^6/s to fit the experiment [27]. The operating temperature is assumed to be 300 K. In this simulation processes, the built-in interface charges due to the spontaneous and piezoelectric polarizations are calculated based on the method proposed by Fiorentini *et al.* [28]. Other material parameters of the semiconductors used in the simulation can be found elsewhere [29].

3. Results and Discussions

Through the APSYS software, we calculate the energy bands for the investigated DUV LED structures as shown in Fig. 2, which shows the difference in the LBs of different designs. Firstly, in comparison to the p-EBL for the common DUV LED, the p-EBLs for DUV LEDs with SLSLBs have the higher effective conduction band barrier height (the effective conduction band barrier height is defined as the energy difference between the conduction band and the quasi-Fermi level to the EBL barrier) and lower effective valence band barrier height (the effective valence band barrier height is defined as the energy difference between the valance band and the quasi-Fermi level). Besides, the comparison among different SLSLBs also shows a special regular. The p-EBL for the SLSLB-I LED has the low conduction band barrier height that is only 771 meV, and it is smaller than 824 meV of the p-EBL for SLSLB-E LED and 852 meV of the p-EBL for SLSLB-D LED. The variation of the valence band barrier height for the p-EBL has an opposite trending, e.g., 399 meV for SLSLB-I LED, 381 meV for SLSLB-E LED, and 366 meV for SLSLB-D LED. The larger effective conduction band barriers for the p-EBL indicates that the electron concentration at the interface

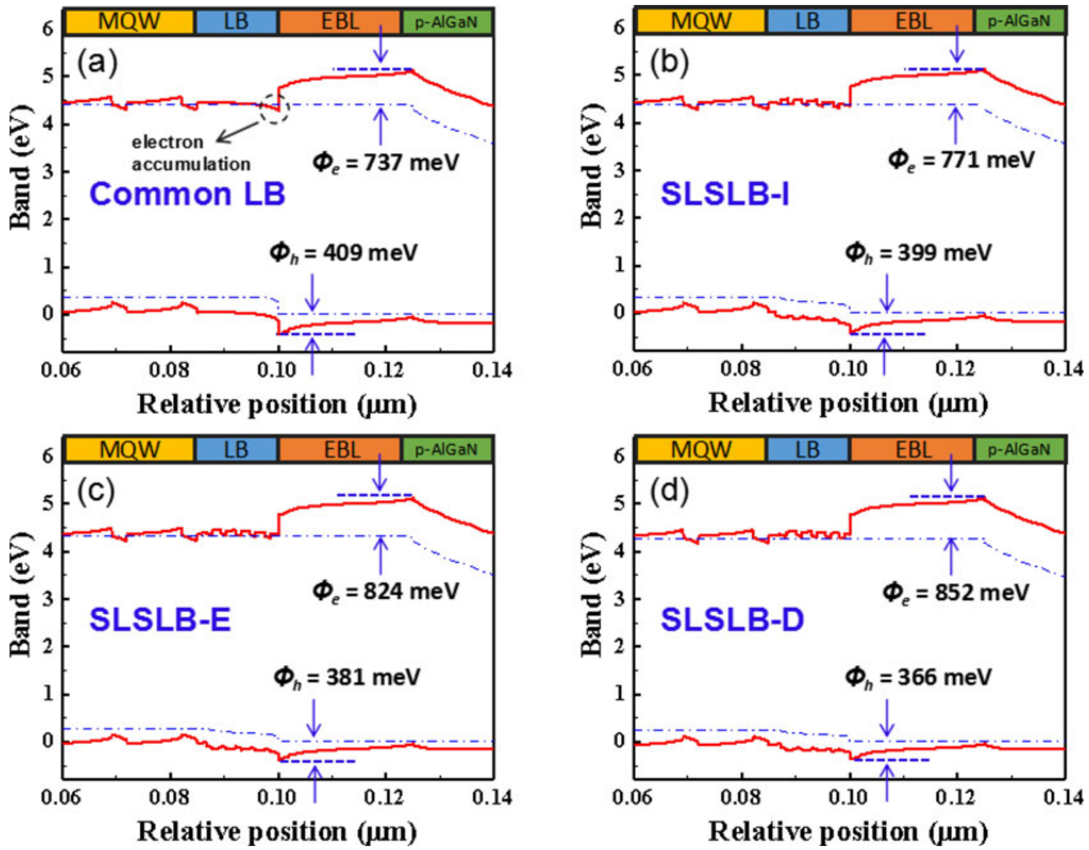

Fig. 2. Energy band diagrams for different structured DUV LED devices with (a) common last barrier, (b) SLSLB-I, (c) SLSLB-E, (d) SLSLB-D. The barrier heights for the conduction band and the balance band of the p-EBL are also marked.

between the LB and the EBL is decreased, and this enables the quasi-Fermi level to more deviate from the conduction band edge.

For further explaining the underlying mechanism for the band diagrams of different SLSLBs, we calculate the profiles for the electron concentrations of LEDs with different last barriers, which are illustrated in Fig. 3. It shows the distribution of electron concentration in the EBL and the p-AlGaN layer (we define the p-EBL and the p-AlGaN layer as the hole injection layer) at the current density of 35 A/cm^2, and we can obtain that the concentration of leakage electron is decreased with the increase of the effective conduction band barrier height for the p-EBL, i.e., the DUV LED with SLSLB-D has the lowest leakage electron concentration. The other SLSLB structures also have a significant reduction in electron leakage, which indicates that the SLSLB structure can effectively suppress the electron leakage. According to the illustration, it is obvious that the average electron concentration decreases from the reference common LED, the SLSLB-I LED, the SLSLB-E LED to the SLSLB-D LED. A low electron concentration makes the quasi-Fermi energy level for electrons apart from the conduction band, thus increasing the effective conduction band of the p-EBL [30], [31]. The finding here are well consistent with Fig. 2. If the electron concentration in the LB region decreases, the effective conduction band barrier height for the p-EBL can be increased and this helps to reduce electron leakage into the p-type hole injection layer.

As has been discussed previously, due to the decrease of effective valence band barrier height for the p-EBL, the hole concentration in the QWs has been remarkably improved for DUV LEDs with SLSLB-I, SLSLB-E and SLSLB-D as shown in Fig. 4(a). Fig. 4(a) also presents the most enhanced hole injection for the DUV LED with the SLSLB-D. On the other hand, lower electron leakage results

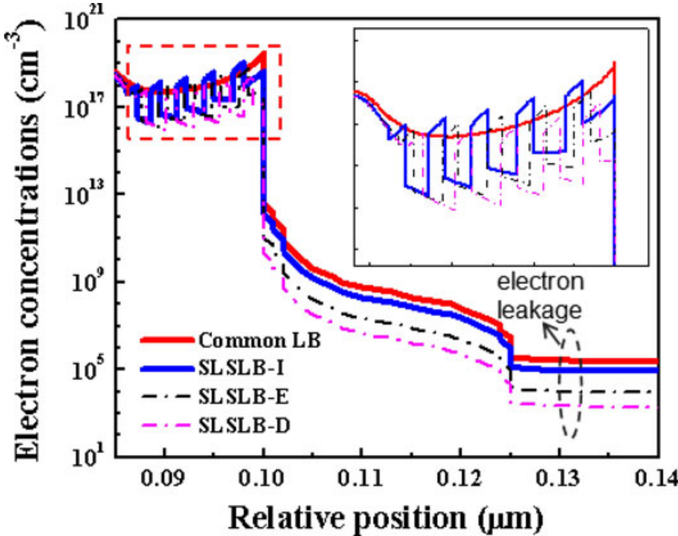

Fig. 3. Electron concentration profiles within different last barriers in the SLSLBs and the hole injection layers for the investigated DUV LEDs, the inset figure is the enlarged electron concentration in the SLSLBs.The hole injection layer comprises the p-EBL and the p-AlGaN layer.

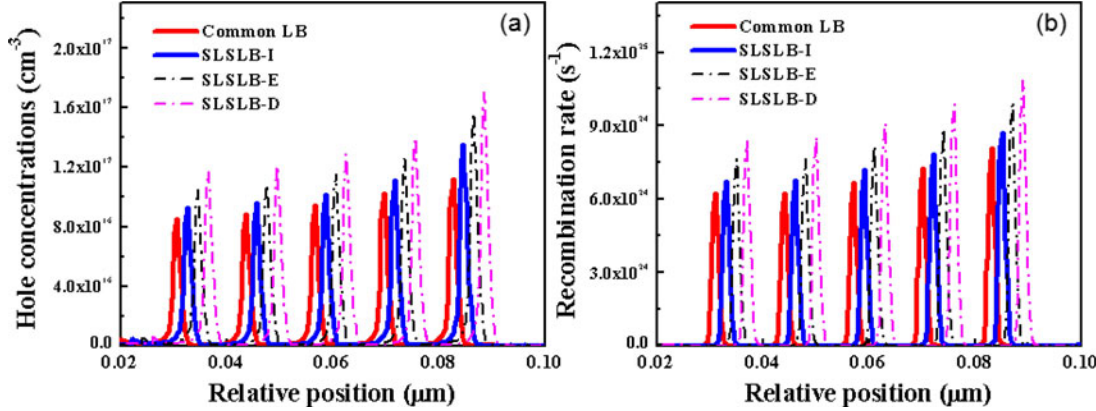

Fig. 4. (a) Hole concentration in the MQW active region. (b) Radiative recombination rate in the MQW layer for the investigated DUV LEDs in this work.

in a smaller consumption of the holes in the p-type injection layer, which also contributes to the higher hole injection efficiency. As has been previously reported, the hole mobility is far lower than the electron mobility in the AlGaN materials [32], [33], and thus the hole concentration in the quantum wells is also lower than the electron concentration by nearly one order of magnitude. As a result, the radiative recombination rate in the quantum well mainly depends on the hole concentration, so the simulation results of the radiative recombination rate that is shown in Fig. 4(b) is similar to Fig. 4(a) in the spatial distribution, such that the radiative recombination rate has the maximum value in the last QW and the minimum in the first QW. In addition, the radiative recombination in the SLSLBs can be ignored due to the negligible hole concentration therein.

Finally, we calculate the optical power and the internal quantum efficiency of the DUV LEDs with different LBs as shown in Fig. 5(a) and (b), respectively. The Reference device with the common LB has the lowest luminous power and the lowest internal quantum efficiency. Besides, the largest efficiency droop (the efficiency droop is defined as by the formula $(IQE_{max} - IQE_{current})/IQE_{max}$.) is also found for the reference device. Fig. 5(a) and (b) also show that the alternative MQLB structures can significantly enhance the optical performance for DUV LEDs. Specifically, the DUV LED with

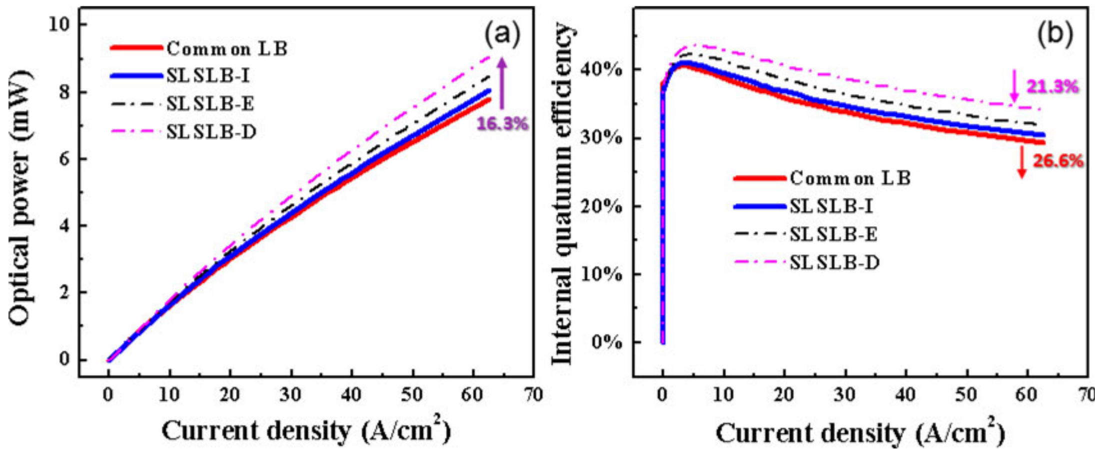

Fig. 5. (a) Optical power and (b) internal quantum efficiency versus the injection current density of different structure UV LEDs.

the SLSLB-D structure has the highest light power when compared with the common LED, such that the optical power is increased by 16.3% at the current density of 60 A/cm^2. At the same time, the LED with SLSLB-D has the efficiency droop pf 21.3% while common LED has the efficiency droop of 26.6% at the current density of 60 A/cm^2. The calculated optical power and the internal quantum efficiency for all the studied DUV LEDs are consistent with the Fig. 4(b).

4. Conclusion

In conclusion, we propose the DUV LEDs structures with SLSLBs for improving the optical performance. We find that the MQLB structure can significantly enhance the optical power and the internal quantum efficiency. Meantime the efficiency droop is also relieved. Furthermore, we further analyze the influence of MQLB barrier thickness on the energy bands. By analyzing the levels of the electron leakage and the hole injection, we confirm that the most improved electron and hole injections can be obtained when the SLSLB-D structure is adopted. We believe that the DUV LEDs by using SLSLB structures are promising for further achieving high efficiency DUV solid-state light sources and meeting the standard of the commercial application.

References

[1] A. Khan, K. Balakrishnan, and T. Katona, *Nature Photon.*, vol. 2, no. 2, pp. 77–84, 2008.
[2] R. Gaska *et al.*, *Appl. Phys. Lett.*, vol. 81, no. 24, pp. 4658–4660, 2002.
[3] M. A. Wurtele *et al.*, *Water Res.*, vol. 45, no. 3, pp. 1481–1489, 2011.
[4] J. Li, J. Y. Lin, and H. X. Jiang, *Appl. Phys. Lett.*, vol. 88, no. 171909, pp. 1–3, 2006.
[5] H. Hirayama, S. Fujikawa, and K. Norihiko, *Electron. Commun. Japan*, vol. 98, no. 5, pp. 1–8, 2015.
[6] H. Hirayama, S. Fujikawa, N. Noguchi, J. Norimatsu, and T. Takano, *Physica Status Solidi(a)*, vol. 206, no. 6, pp. 1176–1182, 2009.
[7] M. Kneissl *et al., Semicond. Sci. Technol.*, vol. 26, no. 014036, pp. 1–6, 2011.
[8] M. Imura *et al.*, *Japanese J. Appl. Phys.*, vol. 45, no. 11, pp. 8639–8643, 2006.
[9] Z. Ren *et al.*, *Physica Status Solidi(c)*, vol. 4, no. 7, pp. 2482–2485, 2007.
[10] J. Piprek, C. Moe, S. Keller, S. Nakamura, and S. P. Denbaars, *Proc SPIE*, vol. 5594, pp. 177–184, 2004.
[11] Zi-Hui Zhang *et al.*, *Appl. Phys. Lett.*, vol. 104, no. 251108, 2014.
[12] J. Piprek and Z. M. Simon Li, *Appl. Phys. Lett.*, vol. 102, no. 131103, 2013.
[13] J. Piprek and Si mon Li, *Opt. Quant. Electron.*, vol. 42, pp. 89–95, 2010.
[14] H. Hirayama, N. Maeda, S. Fujikawa, S. Toyoda, and N. Kamata, *Japanese J. Appl. Phys.*, vol. 53, no. 100209, 2014.
[15] W. Tian *et al.*, *J. Phys. D: Appl. Phys.*, vol. 46, no. 065303, 2013.
[16] Kangkai Tian *et al.*, *Physica Status Solidi Rapid Res. Lett.*, vol. 1700346, pp. 1–5, 2017.
[17] Jun Zhang *et al.*, *IEEE Photon. J.*, vol. 5, no. 4, pp. 1–10, 2013.
[18] M. C. Tsai, S. H. Yen, and Y. K. Kuo, *IEEE Photon. Technol. Lett.*, vol. 22, no. 6, 2010.
[19] C. S. Xia, Z. M. S. Li, W. Lu, Z. H. Zhang, Y. Sheng, and L. W. Cheng, *Appl. Phys. Lett.*, vol. 99, no. 233501, 2011.

[20] S. H. Yen, M. L. Tsai, M. C. Tsai, S. J. Chang, and Y. K. Kuo, *IEEE Photon. Technol. Lett.*, vol. 22, no. 24, 2010.
[21] H. Hirayama, Y. Tsukada, T. Maeda, and N. Kamata, *Appl. Phys. Exp.*, vol. 3, no. 031002, 2010.
[22] Z. H. Zhang *et al.*, *Appl. Phys. Lett.*, vol. 102, no. 193508, 2013.
[23] Shengchang Chen *et al.*, *Appl. Phys. A*, vol. 118, no. 4, pp. 1357–1363, 2014.
[24] M. Katsuragawa *et al.*, *J. Crystal Growth*, vol. 189, no. 190, pp. 528–531, 1999.
[25] S. H. Yen and Y. K. Kuo, *J. Appl. Phys.*, vol. 103, no. 103115, 2008.
[26] W. Tian *et al.*, *Opt. Quant. Electron.*, vol. 45, pp. 381–387, 2013.
[27] C. S. Xia, Z. M. Simon Li, Z. Q. Li, and Y. Sheng, *Appl. Phys. Lett.*, vol. 102, no. 013507, 2013.
[28] V. Fiorentini, F. Bernardini, and O. Ambacher, *Appl. Phys. Lett.*, vol. 80, no. 7, pp. 1204–1206, 2002.
[29] I. Vurgaftman, J. R. Meyer, and L. R. Ram-Mohan, *J. Appl. Phys.*, vol. 89, no. 11, pp. 5815–5875, 2001.
[30] B. C. Lin *et al.*, *Opt. Exp.*, vol. 22, no. 1, pp. 463–469, 2014.
[31] Z. H. Zhang *et al.*, *Appl. Phys. Lett.*, vol. 104, no. 243501, 2014.
[32] P. Kozodoy *et al.*, *Appl. Phys. Lett.*, vol. 75, no. 16, 1999.
[33] M. L. Nakarmi, K. H. Kim, J. Li, J. Y. Lin, and H. X. Jiang, *Appl. Phys. Lett.*, vol. 82, no. 18, pp. 3041–3043, 2003.